

192
7-15-82
PPPL-1908
UC20-F
ME

① I-4223

PPPL-1908

Dr. 687


MASTER

SPATIALLY RESOLVED MEASUREMENTS OF FULLY IONIZED
LOW-Z IMPURITIES IN THE PDX TOKAMAK

By

R.J. Fonck, M. Finkenthal, R.J. Goldston, D.L. Herndon,
R.A. Hulse, R. Kaita, and D.D. Meyerhofer

JULY 1982

PLASMA
PHYSICS
LABORATORY 

PRINCETON UNIVERSITY
PRINCETON, NEW JERSEY

PREPARED FOR THE U.S. DEPARTMENT OF ENERGY,
UNDER CONTRACT DE-AC02-76-CHO-3073.

DISTRIBUTION OF THIS DOCUMENT IS UNLIMITED

Spatially Resolved Measurements of Fully Ionized

Low-Z Impurities in the PDX Tokamak

PPPL--1991

PLASMA 010531

R.J. Fonck, M. Finkenthal,* R.J. Goldston, D.L. Herndon,

R.A. Hulse, R. Kaita, and D.D. Meyerhoffer

Princeton University, Plasma Physics Laboratory

Princeton, New Jersey 08544

Abstract

Radial distributions of fully ionized oxygen and carbon in the PDX tokamak plasma are reported. These ions were detected via radiation emitted in charge-exchange recombination reactions between the impurities and hydrogen atoms from a non-perturbing neutral beam. The C^{6+} and O^{8+} ions are observed out to radii beyond the limiter, which is in contrast to expectations based on coronal equilibrium but consistent with a simple diffusive transport model. Central values of Z_{eff} obtained with these measurements agree with values obtained from plasma resistivity and visible bremsstrahlung measurements.

DISCLAIMER

This document contains information which is proprietary to the U.S. Government and is being furnished to you under a license. It is not to be distributed outside your organization. It is not to be used for advertising or promotional purposes, for creating new publicity for the U.S. Government, or for resale.

*Present Address: The Hebrew University, Racha Institute of Physics,
Jerusalem, Israel

DISTRIBUTION OF THIS DOCUMENT IS UNLIMITED

Low-Z elements such as carbon and oxygen are usually the most abundant impurities in tokamak plasmas. At the central electron temperatures in present large tokamaks ($T_e \sim 1$ to 2 keV), these atoms are fully ionized in the plasma core, and their detection with conventional spectroscopic observations is not possible. The inference of central low-Z impurity behavior from observations of lower charge-state emissions from the plasma edge region will become increasingly uncertain as T_e increases to 5 keV and above in the next generation of tokamak devices, such as TFTR. Thus, direct detection of these fully stripped impurities is necessary. Such measurements are useful in the study of plasma-wall interactions, tests of the effectiveness of divertors and other impurity control techniques, and evaluation of impurity transport models.

We report here the use of optical excitation of low-Z impurities via charge exchange with neutrals from a low power neutral beam to measure spatial distributions of fully stripped carbon and oxygen in Ohmically heated PDX discharges. In addition to allowing a local determination of Z_{eff} in the plasma core where these impurities are fully ionized, these measurements can be used as a probe of low-Z impurity transport effects. Determination of the correct cross-field transport coefficients for impurity ions is an important factor in the reliable calculation of radiated power loss and other impurity effects.

Since an impurity ion is left in an excited state following charge exchange recombination between the ion and a hydrogen atom, the process



is useful for detecting the presence of the ion Z^{+q} (with charge q) by observing the subsequent photon emission from the excited product of the reaction described in Eq. (1). The cross sections for these processes are large ($\sim 10^{15} \text{ cm}^{-2}$), resulting in high emissivities with only a moderate neutral hydrogen density.

Spectral line excitation from this process was observed during neutral beam heating in the ORMAK¹ and ISX-B² tokamaks. Differentiation between the direct effects of charge exchange with the beam and the large plasma parameter changes due to neutral beam heating is sometimes possible by judicious choice of spectrometer location, as was done in ISX-B. Estimates of total oxygen content in ISX-B were obtained by combining the spatially-unresolved charge exchange observations with a simple impurity transport model.

In addition to perturbing the plasma, high power neutral beam heating introduces enough H^0 into the discharge to change the ionization distribution of the impurities themselves. This has been observed on PLT³ and DITE.⁴ To probe the intrinsic impurity behavior, it is thus desirable to employ a non-perturbing source of neutrals to induce reaction, Eq. (1). Central concentrations of fully-stripped carbon in the T-4 tokamak⁵ were determined by using a diagnostic neutral beam as a source of hydrogen atoms. This technique was also used to measure the radial distribution of O^{8+} in the T-10 tokamak.⁶

The experimental apparatus for the measurements on PDX includes a highly collimated diagnostic neutral beam (DNB) which provides neutrals to induce reaction Eq. (1) in the field of view of a grazing incidence spectrometer (Fig. 1). Square wave modulation of the DNB allows discrimination of the desired signal from the background. The DNB, part of the Fast Ion Diagnostic Experiment⁷ on PDX, can vary its angle of injection so that the beam is scanned across the plasma midplane in the line of sight of the spectrometer.

The DNB and the spectrometer are toroidally separated by 36° . The neutral hydrogen atoms in these experiments have a primary energy of 25 keV and a total injected power of 4 to 11 kW. Typical column densities along the line of sight of the spectrometer are 10^8 to 10^9 cm^{-2} , which results in line intensities on the order of 10^{12} to 10^{13} photons/ cm^2 /s/sr. The neutral beam cross section FWHM is 12 cm high and 5 cm wide, while the spatial resolution of the spectrometer in the vertical direction is 2 cm. The spectrometer has two independent detectors on the Rowland circle, each calibrated for absolute intensity measurements via the branching ratio technique. The plasma is scanned by varying the orientation of the neutral beam on a shot-to-shot basis, and the duochromator allows simultaneous monitoring of both carbon and oxygen.

The PDX tokamak⁸ was run with graphite rail limiters for these experiments; the divertor was not activated. The plasma major radius was 147 cm and the nominal limiter radius was 30 cm. The plasma current was 250 kA and the line averaged electron density was $\bar{n}_e = 2.0 \times 10^{13}$ cm^{-3} . Electron density and temperature profiles from a multi-point Thomson scattering system are shown in Fig. 2 for the steady-state portion of the discharge ($100 \text{ ms} \leq t \leq 500 \text{ ms}$). Soft X-ray measurements showed no sawtooth activity in these discharges at the time of injection of the DNB. Shot-to-shot fluctuations of the bulk plasma parameters were $< 5\%$, and the variation of the observed charge exchange signals was $< 10\%$.

An example of the charge exchange induced signal for the OVIII 102Å (3-2) spectral line is shown in Fig. 3. The eight 1 ms-long pulses arise from the 500 Hz square wave modulation of the neutral beam current, which allows phase sensitive detection for weak signals. For this spectral line, the modulated intensity was as high as 100% of the intrinsic line intensity, which is due to

electron and background neutral charge-exchange excitation of O^{7+} along the spectrometer line of sight. Scanning the spectrometer line of sight vertically across the neutral beam showed that no modulated signal appeared outside the beam position, indicating that the observed modulation is due solely to prompt charge-exchange excitation.

Assuming that the modulated neutral hydrogen density and energy distribution from the neutral beam is known, the local impurity density can be derived from the modulated line intensities if the total effective cross sections for excitation of the observed lines are available. For a fully ionized ion of charge Z , the charge-exchange process tends to populate the high- l states with the peak cross sections occurring at n -levels given by $n_{\text{peak}} \sim Z^{0.75}$. Thus both direct charge exchange and cascades from higher n levels contribute to the observed line intensities from the $n=3$ and 4 levels.

We have calculated the cascade-corrected total effective cross section for excitation of various transitions in CVI and OVIII using available cross sections. Theoretical cross sections for charge exchange into a given (n, l) state of CVI have been provided by Shipsey, Browne, and Greene⁹ over the energy range of interest (0.2 to 25 keV/amu). Their values agree well with those of Olson¹⁰ which are only available at 25 keV/amu. In general, it was found that the ratio of effective cross section for excitation of the 4-3 and 3-2 transitions in CVI to the total charge-exchange cross section (i.e., summed over all n, l) was only a weak function of the H° energy. In support of this, the measured ratios of several spectral lines arising from levels of excitation from $n=5$ to $n=3$ for CVI and OVIII showed no variation outside experimental uncertainties with beam species (H° or D°) or plasma radius. The latter can be significant because the beam energy distribution changes somewhat with the radius due to different attenuation of the various energy components.

Except for the values of Salop¹¹ at 25 keV/amu, (n, l) distributions for charge exchange with O^{8+} were not readily available over our energy range. However, in view of the observations above, it is reasonable to assume that the (n, l) distribution due to the $H^+ + O^{8+}$ reaction is independent of energy and is the same as that given by Salop at 25 keV. The large contributions from cascades for excitation of the 3-2 or 4-3 transitions in OVIII result in the uncertainties in the (n, l) distribution among the higher levels, which produces little uncertainty in the effective cross section for these lower transitions. The scaling of the total cross section with energy for O^{8+} was taken from Ryufuku and Watanabe,¹² normalized to the value of Salop at 25 keV.

The line density of hydrogen neutrals from the diagnostic neutral beam was calculated with a 3-D beam attenuation code. The uncertainty in these calculations is estimated to be 10 to 20%. Beam power had been previously calibrated with a calorimeter, and the beam species mix is taken from test stand measurements. The full energy beam neutrals are found to contribute 50% of the intensity of the OVIII 102Å (3-2) transition in the plasma center, while the one half and one third energy components each contribute 20%. The remaining 10% is accounted for by the beam generated thermal (halo) neutrals.

The steady-state ($t = 200$ ms) radial profiles of C^{6+} and O^{8+} are shown in Fig. 4 along with model calculations which are discussed below. The error bars are the uncertainties in the average over the 8 beam pulses. The more reliable data are those at larger major radii (i.e., outside) where the beam has suffered less attenuation. The uncertainties in the absolute density scales in Fig. 4 are dominated by spectrometer calibration uncertainty (30 to 50%), beam power uncertainty, and charge-exchange cross-section uncertainties. Ignoring contributions from all lower charge states (which can only serve to flatten the total impurity density) the levels of $n_{O^{8+}}$ and $n_{C^{6+}}$

are, at most, slightly more peaked than $n_e(r)$, indicating no significant peaking of Z_{eff} on axis.

A noticeable feature of the O^{8+} and C^{6+} profiles in Fig. 4 is that both fully stripped species have appreciable densities beyond the limiter radius at 30 cm. Since the electron temperature at the plasma edge is too low to produce C^{6+} and O^{8+} , impurity transport across the magnetic field in times short compared to the recombination times of 50 to 100 ms must be responsible for the presence of these ions at large radii.

The amount of cross-field transport necessary to account for the observed profiles can be estimated by comparison of the measured O^{8+} and C^{6+} radial distributions to those calculated with a multispecies impurity transport code.¹³ The curves in Fig. 4 show results of steady-state calculations assuming either coronal equilibrium with a constant total impurity density or relatively simple diffusion models ($\Gamma_q = -D \partial n_q / \partial r$). In addition to the usual electron ionization and recombination atomic rates, these calculations include charge-exchange recombination due to the background thermal neutral density. No parallel loss term was included in the scrapeoff region ($r > 30$ cm).

Both the O^{8+} and C^{6+} results show clear deviations from coronal equilibrium, especially at large radii. Results from the TFR tokamak¹⁴ seem to indicate that heavy impurities in the center of the discharge can be described by coronal equilibrium if the uncertainties in the various atomic rates are considered. In addition, the radial distribution of O^{8+} in the T-10 tokamak appears to be in agreement with coronal equilibrium,⁶ albeit with quite large uncertainties in the data. In contrast, results from both the PDX¹⁵ and PLT¹⁶ tokamaks show deviations from coronal equilibrium for heavy impurities. Even with large uncertainties in the thermal neutral density, atomic rate coefficients, and plasma parameters, the O^{8+} and C^{6+} profiles

reported here cannot be reconciled with coronal equilibrium. The measured profiles are in much better agreement with profiles calculated assuming a constant diffusion coefficient of $D = 10^4 \text{ cm}^2/\text{s}$, which is the value obtained from analysis of earlier Sc injection experiments.¹⁵

Uncertainties in various plasma parameters, including n_e , T_e , the thermal neutral density, scrapeoff parallel loss times, and other details, make it difficult to straightforwardly obtain rigorous transport results from the present data. Considering all these uncertainties, a wide range of D ($\sim 5 \times 10^3$ to $2 \times 10^4 \text{ cm}^2/\text{s}$) can give reasonable agreement with the observed profiles. It is clear that there is no strong central pinch effect on these ions. The purely diffusive model used here yields a constant total impurity density with radius in the core region ($r < 30 \text{ cm}$) where the source rate from recycling impurities is negligible. These uncertainties also allow the inclusion of a small inward velocity term in the flux sufficient to yield a roughly constant total impurity concentration with radius. A more detailed transport analysis of these and other measurements will be reported at a later date.

The intensity of the 102\AA line in the absence of the DNB is due to both electron excitation of O^{7+} and charge-exchange recombination of O^{8+} with the background thermal neutrals. The observed ratio of the modulated to steady-state signals at 102\AA is consistent with the transport code results using a nominal thermal neutral density profile $n_{\text{H}^0}(r)$ obtained from a neutral particle transport code¹⁷ [which gives $n_{\text{H}^0}(0) \approx 2 \times 10^7 \text{ cm}^{-3}$]. However, a factor of three uncertainty in $n_{\text{H}^0}(r)$ precludes a reliable determination of the O^{7+} density from the measured 102\AA intensity. The influence of uncertainties in $n_{\text{H}^0}(r)$ on the impurity ionization balance, and hence the calculated O^{8+} profiles, is less pronounced.

Assuming C and O to be the dominant impurity species and taking these ions to be fully stripped in the plasma center, the measured densities give $Z_{\text{eff}} = 2.4 \pm 0.4$ at $r = 0$. The error estimate reflects the range of values obtained using several (i.e., the 3-2 and 4-3) transitions in O^{7+} and C^{5+} . Plasma resistivity measurements give $Z_{\text{eff}} = 2.1 \pm 0.2$ assuming Spitzer resistivity, and visible bremsstrahlung measurements give $Z_{\text{eff}} = 2.2 \pm 0.3$ at the plasma core. The value of Z_{eff} derived from the charge-exchange measurements is thus consistent with these other independently determined values. Unlike these other methods of determining Z_{eff} , the charge-exchange technique gives the added information of the ionic composition of the plasma. Estimates of the abundance of hydrogenic O in the plasma core would raise the quoted Z_{eff} by $< 5\%$. Metallic impurities (principally titanium) were negligible in these discharges.

In summary, we have demonstrated the use of optical excitation of low-Z impurities via charge-exchange recombination as a viable non-perturbing probe of the local densities of fully-stripped low-Z impurities in tokamak plasmas. Central values of Z_{eff} obtained with this technique are in agreement with values obtained via other techniques. The spatial distributions of C^{6+} and O^{8+} in ohmically heated PDX discharges show large deviations from coronal equilibrium, and they are consistent with the results from a diffusion transport code. Ideally, a combination of charge-exchange measurements of the higher ion states and conventional spectroscopic measurements of lower charge states may lead to a detailed evaluation of low-Z impurity transport across r .

Acknowledgments

The authors wish to acknowledge useful discussions with E. Hinnov, D. Post, and S. Suckewer. B. Grek and D. Johnson provided the Thomson scattering profiles for these discharges. H. Towner provided assistance with the beam attenuation calculations. S. Kaye performed the thermal neutral density calculations, and R. Reeves provided the visible bremsstrahlung results. The assistance of K. Bol and the entire PDX group is gratefully acknowledged. This work was supported by U.S. Department of Energy Contract No. DE-AC02-76-CHO-3073.

References

- ¹R.C. Isler, Phys. Rev. Lett. 38 1359 (1977).
- ²R.C. Isler, L.E. Murray, S. Kasai, J.L. Dunlap, S.C. Bates, P.H. Edmonds, E.A. Lazarus, C.H. Ma, and M. Murakami, Phys. Rev. A 24 2701 (1981).
- ³S. Suckewer, E. Hinnov, M. Bitter, R. Hulse, and D. Post, Phys. Rev. A 22 725 (1980).
- ⁴W.H.M. Clark, et al., Nucl. Fusion 22 333 (1982).
- ⁵V.V. Afrosimov, Yu. S. Gordeev, A.N. Zimov'ev, and A.A. Korotov, Sov. J. Plasma Phys. 5 551 (1979).
- ⁶A.N. Zimov'ev, A.A. Korotko, E.R. Krzhizhanovskii, V.V. Afrosimov, and Yu. S. Gordeev, JETP Lett. 32 539 (1980).
- ⁷A. Nudelman, R. Goldston, and R. Kaita, to be published in the J. Vac. Sci. and Technol.
- ⁸D. Meade et al., in Proceedings of the Eighth International Conference on Plasma Physics and Controlled Nuclear Fusion Research, Brussels, Belgium (1980). (IAEA, Vienna, Austria 1981) Vol. I, p. 665.
- ⁹T.A. Green, E.J. Shipsey, and J.C. Browne, Phys. Rev. A23, 546 (1981).
- ¹⁰R.E. Olson, private communication to S. Suckewer.
- ¹¹A. Salop, J. Phys. B: Atom. Molec. Phys. 12, 919 (1979).
- ¹²H. Ryufuku and T. Watanabe, Phys. Rev. A 18 2005 (1978).
- ¹³R.A. Hulse, to be published in Nucl. Tech./Fusion.
- ¹⁴TFR Group, Association Euratom-CEA, Fontenay-aux-Roses, Report EUR-CEA-FC-1033 (1980).
- ¹⁵R. Hulse, K. Brau, J. Cecchi, S. Cohen, M. Finkenthal, R. Fonck, D. Manos, and S. Suckewer, Bull. Am. Phys. Soc. 26 864 (1981).

¹⁶E. Hinnov, in Atomic and Molecular Processes in Controlled Thermonuclear Fusion (1960), Ed. M.R.C. McDowell and A.M. Ferendeci (Plenum, New York) pp. 449-470.

¹⁷S. Tamor, J. Comput. Phys., 40, 104 (1981).

Figure Captions

- Fig. 1. Schematic of experimental apparatus for low-Z impurity diagnostic on PDX.
- Fig. 2. Electron density and temperature profiles from Thomson scattering. $t = 200$ ms.
- Fig. 3. Excitation of OVIII 102Å ($n=3$ to $n=2$) emission by charge exchange with the pulsed diagnostic neutral beam.
- Fig. 4. Radial profiles of fully ionized oxygen and carbon during the steady-state phase of the discharge. Limiter radius is at 30 cm. Closed circles: $R > R_{pl}$. Open circles: $R < R_{pl}$. $R_{pl} = 147$ cm. The solid lines are radial profiles of C^{6+} and O^{8+} calculated from impurity transport code. C.E. = distribution expected from coronal equilibrium assuming a constant impurity density. D = constant impurity diffusion coefficient.

82X0247

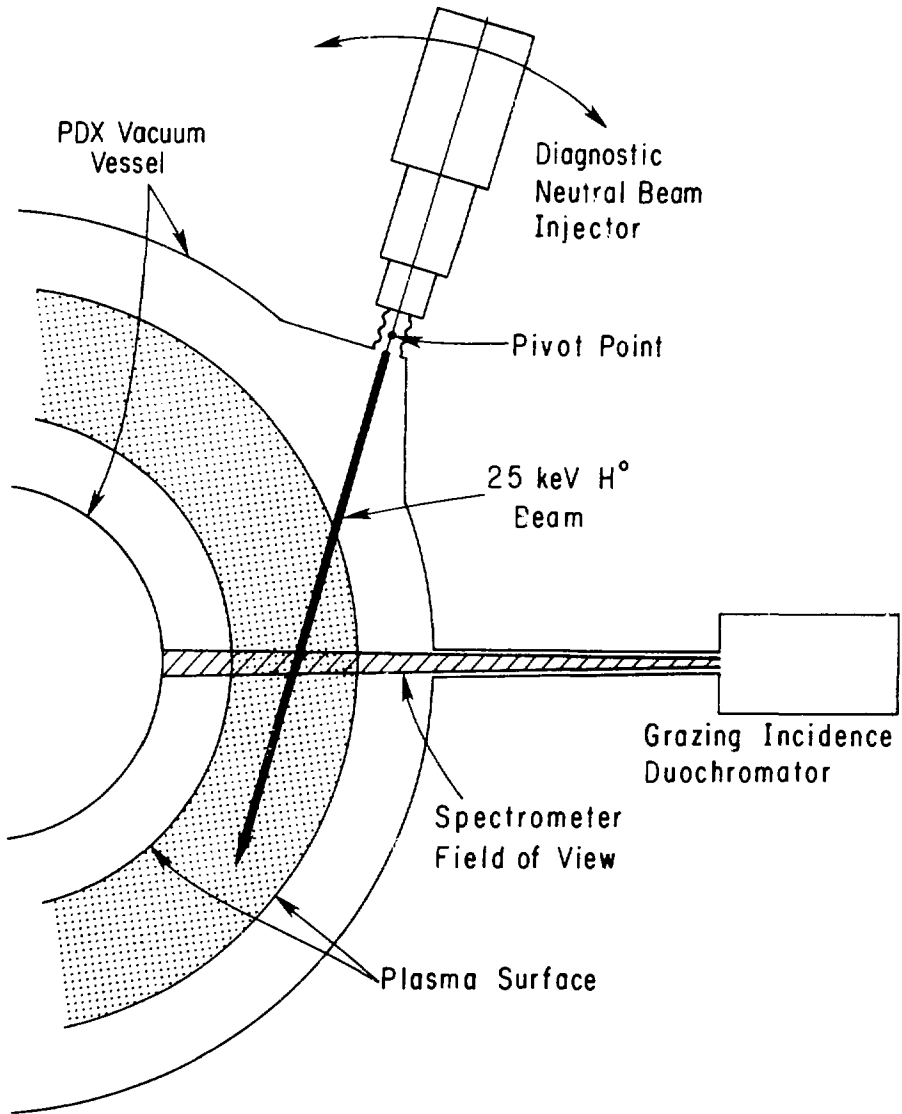


Fig. 1

82X0249

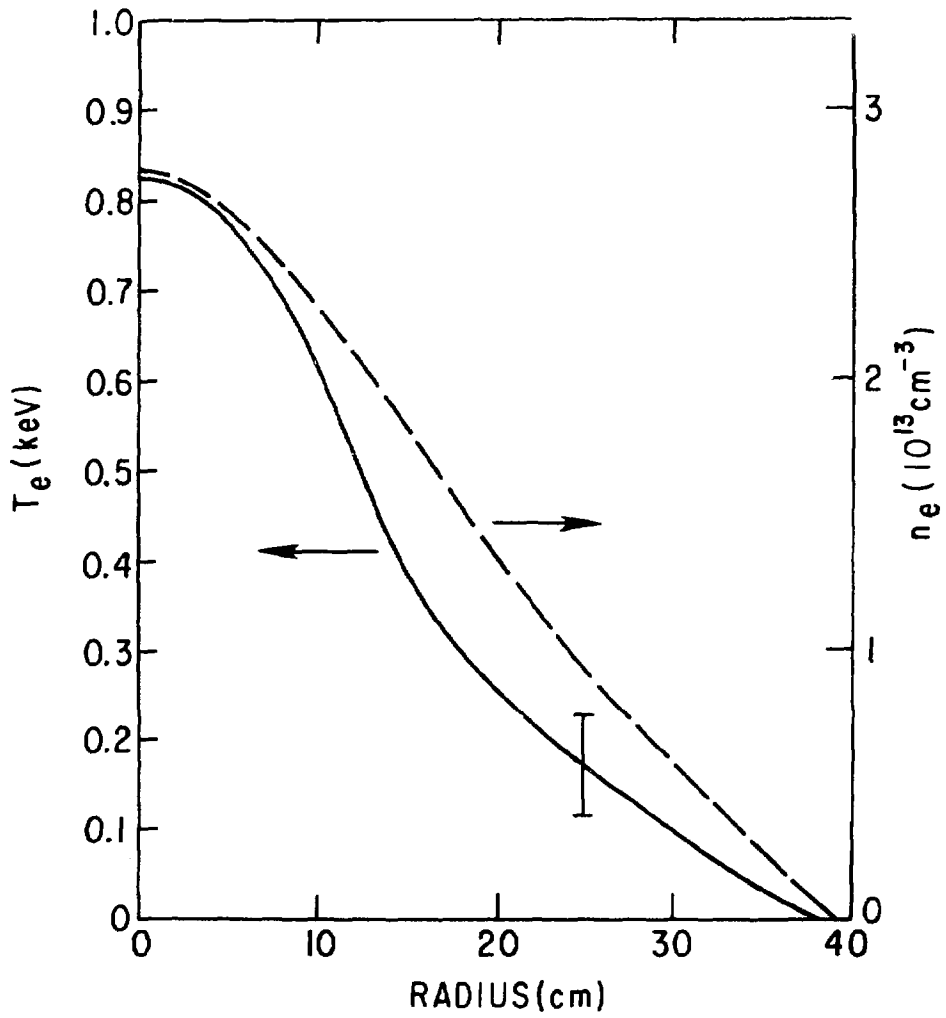


Fig. 2

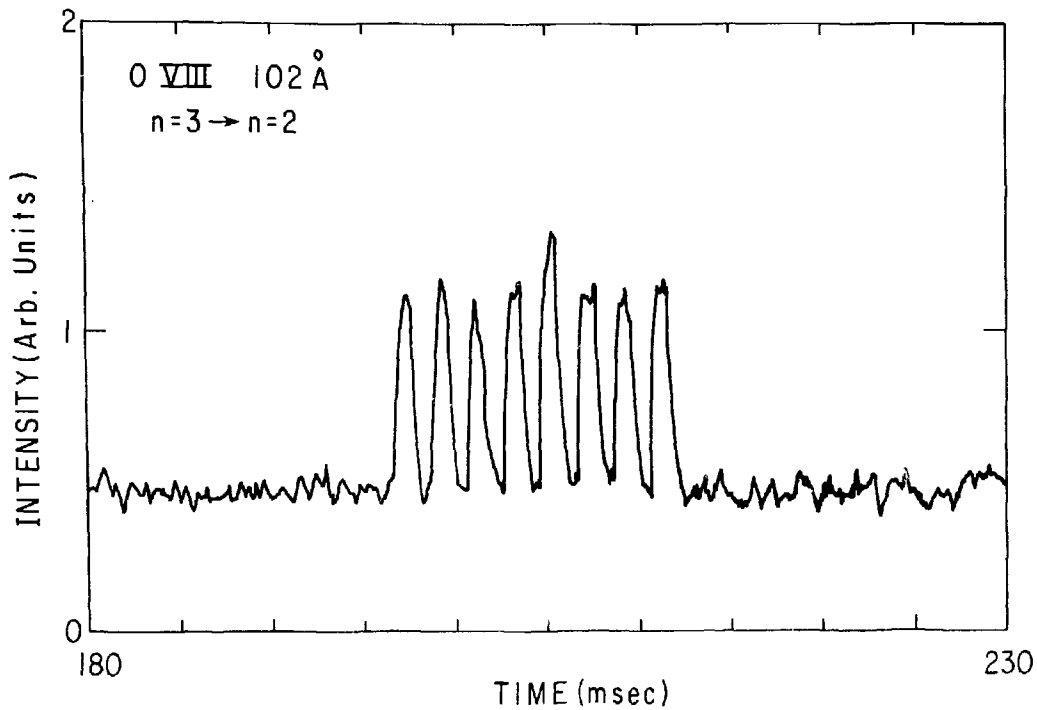


Fig. 3

82X0246

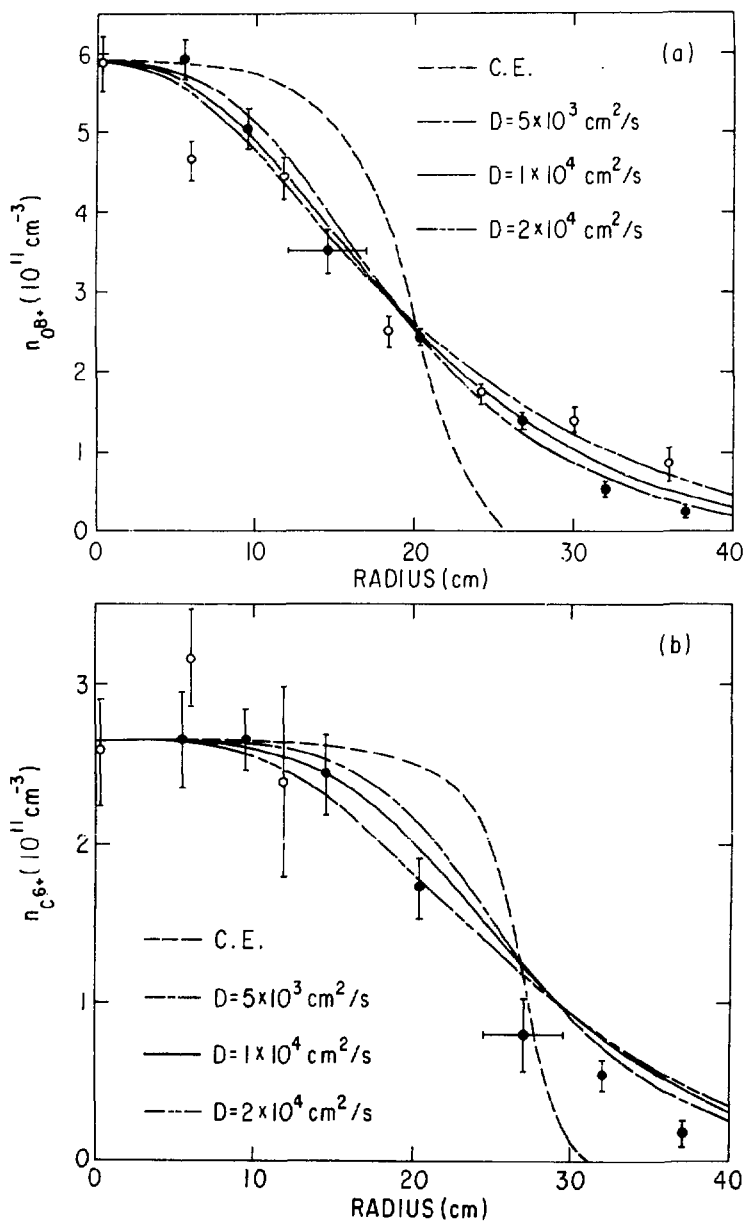


Fig. 4